Journal of Veterinary Cardiology (2021) **34**, 80—92

Journal of Veterinary Cardiology
ESVC

www.elsevier.com/locate/jvc

Ultrasonographic evaluation of the caudal vena cava in dogs with right-sided heart disease☆

T. Fujioka, DVM[a,b], K. Nakamura, PhD[c], T. Minamoto, PhD[d], N. Tsuzuki, PhD[e], J. Yamaguchi, DVM[a], Y. Hidaka, PhD[b,*]

[a] *Asap Animal Clinic, 3597-1 Ganda, Nogata, Fukuoka 822-0001, Japan*
[b] *Laboratory of Veterinary Surgery, Department of Veterinary Medicine, Faculty of Agriculture, University of Miyazaki, 1-1 Gakuen Kibanadai-nishi, Miyazaki 889-2192, Japan*
[c] *Organization for Promotion of Tenure Track, University of Miyazaki, 1-1 Gakuen, Kibanadai-nishi, Miyazaki 889-2192, Japan*
[d] *Evergreen Vet Research & Publication, 2-10-2 Hanaike, Ichinomiya, Aichi 491-0914, Japan*
[e] *Department of Clinical Veterinary Science, Obihiro University of Agriculture and Veterinary Medicine, Inada, Obihiro, Hokkaido 080-8555, Japan*

Received 16 July 2018; received in revised form 17 January 2021; accepted 19 January 2021

KEYWORDS
Canine;
Echocardiography;
Right-sided cardiac function;
Right-sided congestive heart failure;
Tricuspid regurgitation

Abstract *Introduction/objectives:* In humans with impaired right-sided cardiac function, the caudal vena cava (CVC) diameter serves as a marker of venous congestion. This study aimed to investigate whether ultrasonographic CVC variables could identify the presence of right-sided congestive heart failure (R-CHF) in dogs with right-sided heart disease (RHD).
Animals: Fifty client-owned control dogs and 67 dogs with RHD were enrolled. The dogs with RHD were subdivided into the non-R-CHF (n = 43) and R-CHF (n = 24) groups.

☆ A unique aspect of the Journal of Veterinary Cardiology is the emphasis of additional web-based materials permitting the detailing of procedures and diagnostics. These materials can be viewed (by those readers with subscription access) by going to http://www.sciencedirect.com/science/journal/17602734. The issue to be viewed is clicked and the available PDF and image downloading is available via the Summary Plus link. The supplementary material for a given article appears at the end of the page. To view the material is to go to http://www.doi.org and enter the doi number unique to this paper which is indicated at the end of the manuscript.

* Corresponding author.
E-mail address: yhidaka@cc.miyazaki-u.ac.jp (Y. Hidaka).

https://doi.org/10.1016/j.jvc.2021.01.005

Materials and methods: We measured and compared the ultrasonographic CVC variables and echocardiographic variables among the groups. Receiver operating characteristic (ROC) curve analysis was performed to calculate the sensitivity and specificity of the variables at optimal cutoff values.
Results: We obtained the highest accuracies of the ratio of the shortest diameter (SD) of the minimal CVC area to the aorta diameter (Ao) during inspiration [SD(min)/Ao] and of the ratio of SD(min) to the longest diameter of the minimal CVC area during inspiration [LD(min),SD/LD(min)], with high sensitivities, specificities, and an area under the ROC curve greater than 0.925.
Conclusions: In addition to the echocardiographic assessment of right-sided cardiac function, the CVC variables in this study, especially SD(min)/Ao and SD/LD(min), would be useful diagnostic indices for identifying R-CHF in dogs with RHD.

Abbreviations

Ao	aorta
BSA	body surface area
CI	confidence interval
CVC	caudal vena cava
CVP	central venous pressure
IVC	inferior vena cava
LD	longest diameter of the caudal vena cava area
LD max	longest diameter of the maximal caudal vena cava area during expiration
LD min	longest diameter of the minimal caudal vena cava area during inspiration
MMVD	myxomatous mitral valvular disease
PH	pulmonary hypertension
RA	right atrial
RAP	right atrial pressure
R-CHF	right-sided congestive heart failure
RHD	right-sided heart disease
ROC	receiver operating characteristic
RV	right ventricular
RVTX	right ventricular Tei index
SD	shortest diameter perpendicular to the longest diameter of the caudal vena cava area
SD/LD	ratio of SD to LD
SD/LD(min)	Ratio of SD min to LD min
SD max	shortest diameter perpendicular to the longest diameter of the maximal caudal vena cava area during expiration
SD min	shortest diameter perpendicular to the longest diameter of the minimal caudal vena cava area during inspiration
SD (min)/Ao	ratio of SD min to Ao diameter
TAPSE	tricuspid annular plane systolic excursion
TTFE	peak velocity of early diastolic transtricuspid flow
TR	tricuspid regurgitation

Introduction

Impaired right-sided heart function has been reported to be associated with poor prognosis in human patients with various cardiac diseases, such as ischaemic heart disease, dilated cardiomyopathy, mitral regurgitation, and pulmonary embolism [1—7]. Decreased tricuspid annular plane systolic excursion (TAPSE), elevated right ventricular (RV) end-diastolic diameter, and altered peak longitudinal strain of the RV free wall are known to be poor prognostic indicators in human patients with such cardiac diseases [1—4,7].

Right ventricular Tei index (RVTX) and TAPSE are the independent predictors of mortality in dogs with arrhythmogenic RV cardiomyopathy and myxomatous mitral valvular disease (MMVD) [8,9]. Previous studies have shown that various echocardiographic variables can be used to predict left-sided congestive heart failure in dogs with MMVD or dilated cardiomyopathy [10—14]. Echocardiographic variables of the left atrium, such as left atrial size, left atrial strain, and peak early diastolic mitral inflow velocity, are good indicators of prognosis and disease severity in dogs with MMVD [10—13].

Recent studies have shown that several echocardiographic variables of right-sided cardiac function were altered in dogs with pulmonary hypertension (PH), MMVD, or arrhythmogenic RV cardiomyopathy [15—21]. However, only a few studies have investigated the relationship between

echocardiographic variables and the presence of right-sided congestive heart failure (R-CHF) in dogs [20,21].

Most patients with R-CHF demonstrate elevated right atrial (RA) pressure (RAP) and central venous pressure (CVP) [22]. Pressure overload, volume overload, myocardial failure, inflow obstruction, and pericardial disease can all lead to R-CHF [23]. The caudal vena cava (CVC) in dogs, or the inferior vena cava (IVC) in humans, is a vessel with high compliance whose size and shape vary with changes in CVP [24,25]. The diameter of the CVC, or the IVC, is correlated with RAP and CVP [24—26]. In human medicine, a large IVC diameter and low IVC respiratory variability accurately indicate high RAP [27]. Thus, the IVC diameter, IVC respiratory variability, and ratio of the minor to major axes of the IVC area serve as diagnostic markers of R-CHF in human patients with chronic heart failure [26,28,29]. The CVC diameter, ratio of the CVC diameter to the aorta (Ao) diameter, and CVC respiratory variability have been investigated in dogs; however, these studies were not related to heart diseases [24,30—32]. No study has investigated the ratio of the minor to major axes of the CVC area in dogs. In dogs, R-CHF has been diagnosed on the basis of the presence of ascites and a visual confirmation of dilatation of the CVC on ultrasonographic examination [20,21]. However, these evaluations are rather subjective and diagnostic cutoff values of ultrasonographic CVC variables for the assessment of R-CHF have not been investigated in dogs.

In the present study, we aimed to compare the ultrasonographic CVC and echocardiographic variables of right- and left-sided cardiac function between healthy control dogs and dogs with right-sided heart disease (RHD), with and without R-CHF. Furthermore, we aimed to assess the ability of these variables to identify the presence of R-CHF in dogs with RHD.

Animals, materials, and methods

Animals

Client-owned dogs with RHD and clinically healthy dogs were prospectively enrolled into the study between August 2015 and March 2018 at Asap Animal Clinic. The study was approved by the Animal Ethics Committee of the University of Miyazaki, and all clients were informed of the details of the study and provided written consent forms.

Dogs were determined as clinically healthy (group 1) based on the absence of any clinical signs, absence of abnormal findings on physical examination, electrocardiography, echocardiography, and abdominal ultrasonography, negative results of heartworm antigen test, and absence of medication history within 4 weeks before study enrolment.

Dogs diagnosed with RHD underwent the following diagnostic tests: physical examination, heartworm antigen test, abdominal ultrasound, conventional transthoracic echocardiography, and electrocardiography. Dogs were enrolled into the RHD group if they had any one of the following conditions based on the diagnostic tests: heartworm disease with/without PH, PH of unknown origin, left-sided heart disease with PH, or pulmonary stenosis. Dogs with RHD were included in this study regardless of their cardiac medication history. Dogs with RHD were excluded if they had any one of the following conditions that are not related to primary RHD: the presence of pericardial disease, RV inflow obstruction due to a cardiac tumour, or left-sided heart disease without PH.

The RHD group was subdivided into two groups: RHD without R-CHF (group 2) and RHD with R-CHF (group 3). If ascites was not present, a dog was categorised into group 2. If abdominal fluid was observed on abdominal ultrasound, peritoneal fluid analysis via paracentesis was performed to confirm transudative ascites and blood test (i.e., complete blood count and plasma chemistry panel) was performed to rule out hypoalbuminemia ($<$1.5 g/dL; normal range: 2.5—4.1 g/L) or any non-cardiac conditions that can cause transudative ascites (e.g., liver failure). If transudative ascites related to RHD was present based on these examinations, the dog was categorised into group 3.

PH was defined as a peak tricuspid regurgitation (TR) jet velocity greater than 2.8 m/s and/or a pulmonary regurgitation jet velocity greater than 2.2 m/s [33] on echocardiologic examination. The severity of PH was classified into the following three categories based on the TR pressure gradient: mild PH (TR pressure gradient between 31.4 and 50 mmHg), moderate PH (50—75 mmHg), and severe PH ($>$75 mmHg) [33]. Pulmonary stenosis was defined as a spectral Doppler pulmonary velocity greater than 1.6 m/s on echocardiographic examination [34].

Ultrasonographic measurements of aorta and CVC variables

Views

All ultrasonographic examinations were performed by a single experienced sonographer (TF).

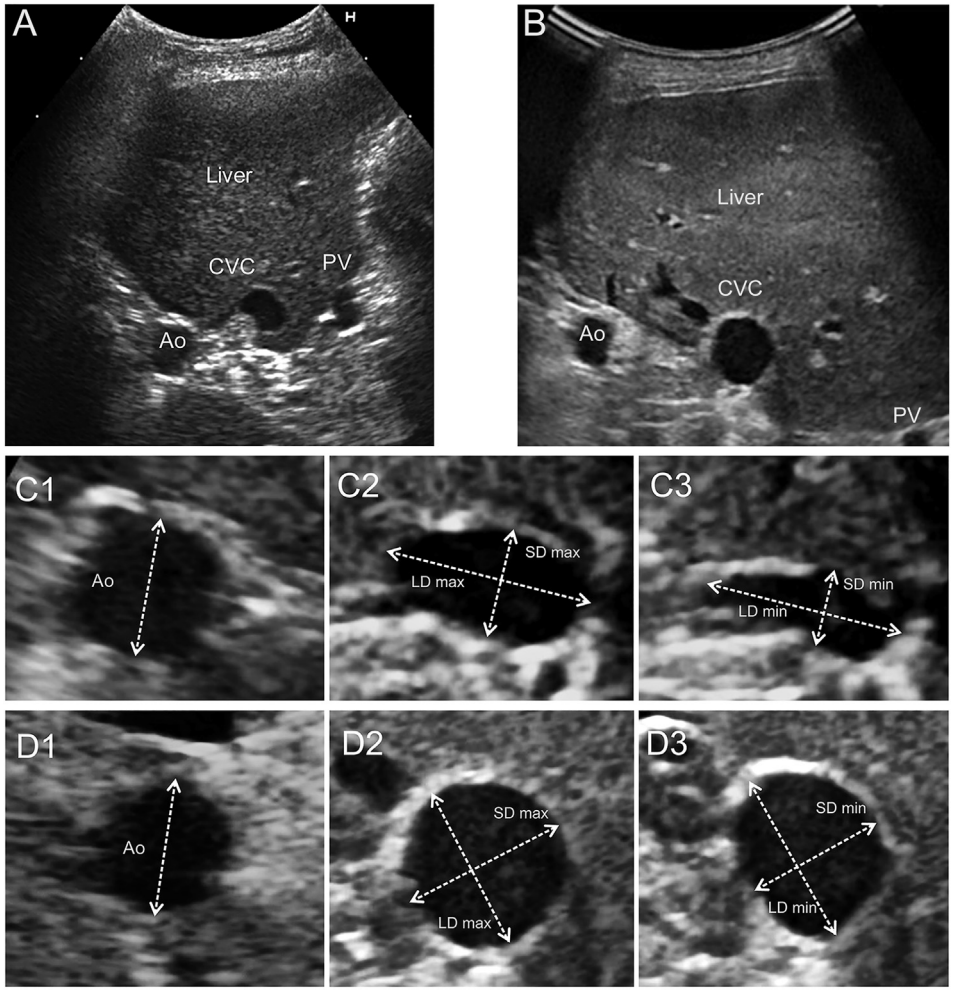

Figure 1 Transverse ultrasonographic images obtained via the right intercostal space of a healthy dog (A, C1—3) and a dog with right-sided congestive heart failure (R-CHF) (B, D1—3). A short-axis ultrasonographic zoomed image of the maximal caudal vena cava (CVC) during expiration (C2, D2) and minimal CVC during inspiration (C3, D3). The arrows indicate the longest diameter (LD) and shortest diameter (SD) of the CVC area. The SD was defined as a diameter perpendicular to the LD. Aorta (Ao) diameter measurements are also shown (C1, D1). LD max: LD of the maximal CVC area during expiration; LD min: LD of the minimal CVC area during inspiration; PV: portal vein; SD max: SD of the maximal CVC area during expiration; SD min: SD of the minimal CVC area during inspiration.

The measurements were recorded using an ultrasound scanner,[f,g] with a 2—8-MHz convex probe.[h,i] All dogs were manually restrained without sedation or anaesthesia in left lateral recumbency. On the basis of a previous study, a probe was placed in a transverse position at the 10th to 12th right dorsolateral intercostal space to acquire the CVC and Ao measurements [30—32]. If lung interference was present, the transducer was moved one intercostal space caudally. If the right kidney was identified, the transducer was moved one intercostal space cranially. A transverse plane of the CVC and Ao was obtained where they were perpendicular to the longitudinal plane and the CVC area was not falsely too large owing to angulation. The liver was used as an acoustic window to obtain clear views of the CVC and Ao (Fig. 1-A, B). Magnified ultrasound images of CVC and Ao were recorded using the zoom mode of the ultrasound device. All measurements were obtained with the dogs lying motionless and breathing quietly.

[f] Hitachi Hi Vision 900, Hitachi Medical Corporation, Tokyo, Japan.
[g] Arietta, Hitachi-Aloka Medical, Ltd., Tokyo, Japan.
[h] EUP-C532, Hitachi Medical Corporation, Tokyo, Japan.
[i] C35, Hitachi-Aloka Medical, Ltd., Tokyo, Japan.

Aorta

Transverse ultrasonographic images of the Ao were obtained when the Ao and CVC were visible in the same cross section. The largest Ao diameter was measured using a frame in which a maximum subjective dimension was observed during the systolic phase of the cardiac cycle (Fig. 1-C1, D1). The Ao diameters were measured from three consecutive cardiac cycles. The mean values were calculated.

Caudal vena cava

The area of the CVC changes depending on respiratory phases. It reaches a minimum during inspiration and a maximum during expiration. Ultrasonographic images of the CVC were obtained at the junction of the hepatic vein during expiration and inspiration. A cross-sectional short-axis plane of the CVC perpendicular to the long-axis was obtained when the area was the smallest and not falsely too large because of angulation. The respiratory phase was determined according to the ultrasonographic lung-sliding sign and careful observation of the respiratory motion by the restrainer.

Diameter of the minimal CVC area during inspiration

An ultrasonographic image of the minimal CVC area during inspiration was obtained. The longest diameter of the CVC area (LD min) and the shortest diameter (SD min) perpendicular to the LD min were measured (Fig. 1-C3, D3) [29,35].

Diameter of the maximal CVC area during expiration

An ultrasonographic image of the maximal CVC area during expiration was obtained. The longest diameter of the CVC area (LD max) and the shortest diameter (SD max) perpendicular to the LD max were measured (Fig. 1-C2, D2) [29,35]. For both the minimal and maximal CVC areas, the LD and SD during three consecutive respiratory cycles were measured and the mean of three measurements was calculated for each variable.

The ratio of the shortest diameter of the CVC area to the longest diameter of the CVC area, the ratio of the shortest diameter of the CVC area to the aorta diameter and CVC respiratory variability

The ratios of SD max to LD max and ratio of SD min to LD min [SD/LD(min)] as well as those of SD max to Ao diameter and SD min to Ao diameter [SD(min)/Ao] were calculated. CVC respiratory variability was defined as [(SD max − SD min)/SD max × 100%].

Conventional echocardiographic variables

The same sonographer (TF) performed all echocardiographic examinations using an ultrasound scanner[f,g] with a 2—9-MHz sector probe.[h,i] The dogs were gently restrained in right and left lateral recumbency without sedation.

TR severity

The peak systolic TR jet velocity was measured using continuous-wave Doppler from the echocardiographic view with the highest velocity. The severity of TR was categorised into three levels (mild, moderate, and severe) based on the size of the TR jet on colour flow imaging and a continuous-wave Doppler envelope of a TR jet in the left-sided apical four-chamber view. The TR was considered mild if a thin TR colour Doppler jet adjacent to the valve closure and a faint parabolic continuous-wave spectral profile were detected. The TR was considered moderate when an intermediate TR colour Doppler jet and a dense parabolic continuous-wave spectral profile on a continuous-wave Doppler were observed. The TR was considered severe if a very large TR jet reaching the opposite RA wall on a colour Doppler and a triangular contour TR jet signal on a continuous-wave Doppler were detected [20].

Pulmonary artery acceleration time to ejection time

The ratio of the pulmonary artery acceleration time to the ejection time was measured from a standard right-sided parasternal short-axis view at the heart base optimized for the pulmonary artery using pulsed-wave Doppler [33].

RA area index

The RA area from a left-sided apical four-chamber view was assessed. The RA area was obtained by tracing from the lateral aspect of the tricuspid annulus to the septal aspect, following the RA endocardium at the end of ventricular systole [20]. The body surface area (BSA) was calculated using the following formula: $BSA = 0.101 \times \text{body weight (kg)}^{2/3}$ [20]. The RA area indexed to the BSA (RA area index) was calculated using the following formula: RA area index (cm^2/m^2) = maximal RA area (cm^2)/BSA (m^2).

RV fractional area change

The RV fractional area change was measured from the left-sided apical four-chamber view. The RV area measurements were obtained by tracing the RV endocardial border at end-systole and end-diastole while tracing the border to exclude the

papillary muscles from the tracing. The fractional area change percentage was calculated as follows: (RV end-diastolic area − RV end-systolic area)/RV end-diastolic area × 100% [36].

Transtricuspid inflow velocity

In the left-sided apical four-chamber view, we detected the peak velocity of early diastolic transtricuspid flow (TTFE) and late diastolic transtricuspid flow. We measured the peak systolic velocity of the lateral tricuspid annular motion, as well as the peak early and late diastolic velocities of the lateral tricuspid annular motion as determined using pulsed-wave tissue Doppler imaging. The ratio of TTFE to the peak velocity of early diastolic tricuspid annular motion determined using pulsed-wave Doppler was calculated.

Normalised TAPSE

We measured TAPSE from an M-mode recording with an M-mode cursor carefully aligned parallel to the RV free wall using the left-sided apical four-chamber view. We calculated the normalised TAPSE as follows: normalised TAPSE = TAPSE/[body weight (kg)$^{0.33}$] [37].

Right ventricular Tei index

Using a dual pulsed-wave Doppler system, the RVTX was calculated as the sum of the isovolumic contraction time and the isovolumic relaxation time divided by the RV ejection time [38]. We acquired left-sided parasternal short-axis images using dual-phase pulsed-wave Doppler and obtained tricuspid inflow and pulmonary arterial flow spectra during the same cardiac cycle.

Normalised left ventricular internal dimension in diastole

In assessing the left-sided heart, we measured the left ventricular internal diameter at end-diastole on an M-mode echocardiogram in the right-sided parasternal short-axis view. We calculated the normalised left ventricular internal dimension in diastole using the following equation: normalised left ventricular internal dimension in diastole = left ventricular internal diameter at end-diastole (cm)/[body weight (kg)]$^{0.294}$ [39].

Mitral annulus velocity on Doppler tissue imaging

The early and late diastolic transmitral inflow velocities were measured in the left-sided apical four-chamber view using a pulsed-wave Doppler system. We also measured the peak systolic and the early and late diastolic velocities of the longitudinal left ventricular wall motion at the septal and lateral mitral annulus with pulsed-wave tissue Doppler imaging.

Statistical analysis

The chi-square test or Fisher's exact test was used to compare demographic categorical variables. All continuous variables were tested for the normality of distribution of the data using the Shapiro–Wilk test. Normally distributed data are presented as mean ± standard deviation; non-normally distributed data are presented as median and interquartile range. A p-value less than 0.05 was considered significantly different.

When comparing variables between two groups, in addition to the Shapiro–Wilk test, the F-test of equality of variances was used to assess the homogeneity of variances. If the data were normally distributed and had the same variance, Student's t-test was used. If the data were not normally distributed, the Mann–Whitney *U*-test was used. When comparing continuous variables among the three groups, Bartlett's test was used to assess the homogeneity of variances. One-way analysis of variance was used if both the assumptions of a normal data distribution and homogeneity of variances were verified. The Kruskal–Wallis test was used if the assumption of a normal data distribution and/or the assumption of homogeneity of variances was not verified. Post hoc multiple comparisons among the three groups were performed using Bonferroni correction, and a p-value less than 0.0167 was considered statistically significant.

The relationship between body weight and Ao diameter and the relationship between body weight and CVC variables in group 1 were assessed using Spearman's rank correlation coefficient analysis. A p-value less than 0.006 was considered statistically significant to reduce the risk of a type 1 error.

Receiver operating characteristic (ROC) curve analysis was performed to calculate the sensitivity and specificity of the measured ultrasonographic CVC and echocardiographic variables at optimal cutoff values to identify the presence of R-CHF in dogs with RHD (group 2 and 3). The area under the ROC curve was used to assess the diagnostic accuracy for identifying R-CHF in dogs with RHD. All statistical analyses were performed using commercial software packages.[j,k]

[j] The R Foundation for Statistical Computing, version 2.13.0, Vienna, Austria.

[k] JMP Pro, version 12.0.1, SAS Institute Inc., Cary, NC, USA.

Table 1 Signalment, clinical status of cardiovascular diseases, medication history, and causes of right-sided heart disease of dogs included in the study.

Variables		Healthy Group	RHD group		Overall p-value
		Group 1	Group 2	Group 3	
Total number	n	50	43	24	
Age (years)	Median [IQR]	4 [1.5–8][a]	12 [10–13.5][b]	12 [9–14][b]	<0.001
Sex	Male/female	25/25	25/18	12/12	0.698
Body weight (kg)	Median [IQR]	5.9 [3.8–9.8][ab]	5.0 [3.8–8.8][a]	8.7 [7.4–11.8][b]	0.017
TR grade	Mild/moderate/severe (n)	–	11/19/9[a]	1/5/18[b]	<0.001
Presence of PH	Absent/present	–	3/40	1/23	0.547
Severity of PH estimated from TRPG	Mild/moderate/severe (n)	–	18/16/5[a]	3/10/10[b]	0.002
Medication	Receiving medication (n)	–	19	11	0.650
	ACE inhibitor (n)	–	10	6	0.680
	Pimobendan (n)	–	12	4	0.233
	Loop diuretics (n)	–	4	6	0.087
	Sildenafil (n)	–	5	4	0.830
	Spironolactone (n)	–	0	1	0.358
	Amlodipine (n)	–	4	2	0.633
Cause of RHD	HWD with PH (n)	–	9	13	0.006
	MMVD complicated with HWD and PH (n)	–	3	1	0.547
	MMVD complicated with PH (n)	–	15	5	0.177
	PH of unknown origin (n)	–	13	4	0.176
	Pulmonary stenosis Mild/moderate/severe (n)	–	2/1/0	0/0/1	0.678

Values with different superscripted letters (a and b) indicate significant differences between groups ($p<0.0167$).
ACE, angiotensin-converting enzyme; HWD, heartworm disease; IQR, interquartile range; MMVD, myxomatous mitral valvular disease; PH, pulmonary hypertension; RHD, right-sided heart disease; TR, tricuspid regurgitation; TRPG, tricuspid regurgitation pressure gradient.

Results

Study group characteristics in dogs with RHD and in healthy dogs

In total, 117 dogs were enrolled: 50 healthy dogs (group 1) and 67 dogs with RHD. Among the dogs with RHD, 43 dogs did not have R-CHF (group 2) and 24 dogs had R-CHF (group 3). Table 1 shows the signalment, clinical status of cardiovascular diseases, medication history, and causes of RHD. The proportions of pure breeds to mixed breeds were 45/5 in group 1, 34/9 in group 2, and 11/13 in group 3. The distribution of small-sized (<10 kg), medium-sized (10 to <30 kg), and large-sized (≥30 kg) dogs was 38/11/1 in group 1, 38/5/0 in group 2, and 15/9/0 in group 3 (the list of breeds is provided in Supplementary Table A available in Supplementary Material online). Dogs in group 1 (median [interquartile range]: 4 [1.5–8] years) were significantly younger than those in group 2 (12 [10–13.5] years) and 3 (12 [9–14] years) (both $p<0.001$). The body weight significantly differed among the three groups ($p=0.017$); however, dogs in group 3 (median [interquartile range]: 8.7 [7.4–11.8] kg) had a significantly greater body weight than dogs in group 2 (5.0 [3.8–8.8] kg, $p=0.003$). The sex distribution did not significantly differ among the three groups ($p=0.698$).

In the 67 dogs with RHD (groups 2 and 3), the causes of RHD (Table 1) were heartworm disease with PH (n = 22), MMVD complicated with PH (n = 20), PH of unknown origin (n = 17), MMVD complicated with heartworm disease and PH (n = 4), and pulmonary stenosis (n = 4). The number of dogs with heartworm disease (n = 13) in group 3 was significantly higher than that in group 2 (n = 9) ($p=0.006$). In total, 94.0% of the dogs (63/67) with RHD (group 2 and 3) were diagnosed with PH based on the TR and/or pulmonary regurgitation pressure gradient. With respect to the severity of PH based on the TR pressure gradient, group 2 had 18 dogs with mild PH (mean ± standard deviation: 40.7 ± 5.1 mmHg), 16

dogs with moderate PH (59.7 ± 6.9 mmHg), and five dogs with severe PH (94.3 ± 13.7 mmHg). Group 3 had three dogs with mild PH (39.6 ± 8.0 mmHg), ten dogs with moderate PH (60.7 ± 8.6 mmHg), and ten dogs with severe PH (95.6 ± 13.9 mmHg). One dog (1/63) was diagnosed with PH based on a pulmonary arterial valve regurgitation gradient of 41 mmHg because of the absence of a TR jet. No significant differences were observed in the type of cardiac medications between group 2 and 3 (p=0.650, Table 1).

Ultrasonographic CVC variables and conventional echocardiographic variables in dogs with RHD and in healthy dogs

The ultrasonographic CVC variables and echocardiographic variables of the right- and left-sided heart are summarised in Table 2. The SD max, SD min, ratio of SD max to Ao diameter, SD(min)/Ao, ratio of SD max to LD max, and SD/LD(min) were significantly higher in dogs in group 3 than in healthy dogs (group 1, all $p<0.001$) and dogs in group 2 (all $p<0.001$). The CVC respiratory variability in group 3 was significantly lower than that in group 1 ($p<0.001$) and group 2 ($p<0.001$). With respect to the echocardiographic variables of the right-sided heart, the peak TR velocity and peak pulmonary regurgitation velocity in group 3 were significantly higher than those in group 2 (Table 2).

Significant differences between groups 1 and 3, as well as between group 2 and 3 were found (Table 2) in the RA area index ($p<0.001$ and $p<0.001$, respectively), RVTX ($p<0.001$ and $p<0.001$, respectively), TTFE ($p<0.001$ and $p<0.001$, respectively), ratio of TTFE to the peak velocity of early diastolic tricuspid annular motion as determined by pulsed-wave Doppler ($p<0.001$ and $p<0.001$, respectively), RV fractional area change ($p<0.001$ and $p=0.001$, respectively), normalised TAPSE ($p<0.001$ and $p<0.001$, respectively), and peak velocity of systolic lateral tricuspid annular motion as determined by pulsed-wave Doppler ($p<0.001$ and $p=0.002$, respectively). With respect to the left-sided heart, significant differences between groups 1 and 3, as well as between group 2 and 3 were found in the normalised left ventricular internal dimension in diastole value ($p=0.002$ and $p=0.001$, respectively) and late diastolic velocities of the longitudinal left ventricular wall motion at the septal mitral annulus with pulsed-wave tissue Doppler ($p=0.006$ and $p=0.005$, respectively).

Correlation analyses between body weight and aorta diameter and between body weight and CVC variables in the healthy dogs

The results of correlation analyses between body weight and Ao diameter/CVC variables in group 1 are summarised in Supplementary Table B, available in Supplementary Material online. Aorta diameter ($r = 0.922$, $p<0.001$), SD max ($r = 0.872$, $p<0.001$) and SD min ($r = 0.723$, $p<0.001$) had strong positive correlations with body weight.

No significant correlations were found between body weight and the following CVC variables: ratio of SD max to Ao diameter ($r = 0.264$, $p=0.064$), SD min/Ao ($r = 0.287$ $p=0.043$), ratio of SD max to LD max ($r = 0.136$, $p=0.346$), SD/LD (min) ($r = 0.263$, $p=0.065$), and CVC respiratory variability ($r = -0.184$, $p=0.202$).

Diagnostic accuracy of ultrasonographic CVC and echocardiographic variables for identifying right-sided congestive heart failure in dogs with RHD.

The results of the ROC curve analyses are available in Supplementary Table C in Supplementary Material online. Ratio of SD min to Ao diameter at a cutoff value of 0.957 identified the presence of R-CHF in dogs with RHD with a sensitivity of 75.0% (95% confidence interval [CI]: 53.3—90.2%), a specificity of 88.4% (95% CI: 74.9—96.1%), and an area under the ROC curve of 0.928 (95% CI: 0.870—0.987). In addition, SD/LD(min) at a cutoff value of 0.665 identified the presence of R-CHF in dogs with RHD with a sensitivity of 91.7% (95% CI: 73.0—99.0%), a specificity of 83.7% (95% CI: 69.3—93.2%), and an area under the ROC curve of 0.925 (95% CI: 0.865—0.986).

Discussion

Our results showed that several ultrasonographic CVC variables and echocardiographic variables related to the right- and left-sided heart functions significantly differed between dogs with RHD without R-CHF and dogs with RHD with R-CHF. Most ultrasonographic CVC variables in this study would be useful echocardiographic variables to identify the presence of R-CHF in dogs with RHD.

Ultrasonographic examination of the IVC is a routine, non-invasive diagnostic method of estimating RAP and CVP in humans [26,40]. The CVC variables, such as the ratio of SD to Ao diameter

Table 2 Ultrasonographic caudal vena cava variables and echocardiographic variables from 117 dogs.

Variables	Healthy group	n	RHD group				Overall p-value
	Group 1		Group 2	n	Group 3	n	
Ao diameter (mm)	7.5 [6.4–8.7]^{a}	50	7.4 [6.0–9.3]^{a}	43	8.2 [6.9–9.6]^{a}	24	0.372
SD max (mm)	5.7 [4.5–6.9]^{a}	50	5.8 [4.6–7.6]^{a}	43	10.5 [8.7–11.7]^{b}	24	<0.001
SD min (mm)	3.9 [3.0–4.8]^{a}	50	3.5 [2.5–5.5]^{a}	43	8.5 [7.6–10.3]^{b}	24	<0.001
SD max/Ao	0.74 [0.66–0.82]^{a}	50	0.82 [0.66–1.03]^{a}	43	1.24 [1.09–1.40]^{b}	24	<0.001
SD min/Ao	0.51 [0.41–0.59]^{a}	50	0.47 [0.35–0.77]^{a}	43	1.06 [0.97–1.13]^{b}	24	<0.001
SD/LD (max)	0.54 [0.49–0.61]^{a}	50	0.66 [0.55–0.76]^{b}	43	0.90 [0.83–0.95]^{c}	24	<0.001
SD/LD (min)	0.39 [0.30–0.46]^{a}	50	0.43 [0.32–0.60]^{a}	43	0.82 [0.72–0.89]^{b}	24	<0.001
CVC respiratory variability (%)	33.8 [23.2–39.4]^{a}	50	32.7 [23.8–50.6]^{a}	43	12.7 [10.2–15.7]^{b}	24	<0.001
Peak TR velocity (m/s)	NA		3.57 [3.24–3.98]^{a}	39	4.22 [3.66–4.91]^{b}	24	0.002
Peak PR velocity (m/s)	NA		2.85 ± 0.62^{a}	12	3.37 ± 0.47^{b}	12	0.032
TAPSE (cm)	1.02 [0.84–1.22]^{a}	50	1.02 [0.86–1.20]^{a}	40	0.99 [0.82–1.10]^{a}	20	0.684
nTAPSE	0.56 ± 0.06^{a}	50	0.59 ± 0.11^{a}	40	0.47 ± 0.09^{b}	20	<0.001
RA area index (cm^2/m^2)	7.55 [6.63–8.20]^{a}	50	9.62 [8.42–12.42]^{b}	40	19.42 [16.00–23.83]^{c}	20	<0.001
RV FAC (%)	54.9 ± 7.9^{a}	50	52.4 ± 13.7^{a}	40	40.2 ± 12.3^{b}	21	<0.001
RV S′ (cm/s)	15.4 ± 4.2^{a}	50	14.4 ± 4.9^{a}	42	10.7 ± 3.7^{b}	22	<0.001
RV E′ (cm/s)	11.0 ± 3.0^{a}	50	9.9 ± 2.9^{a}	42	10.0 ± 3.4^{a}	22	0.212
RV A′ (cm/s)	12.6 ± 3.7^{a}	50	13.9 ± 5.0^{a}	42	11.5 ± 5.5^{a}	22	0.134
RVTX	0.23 [0.18–0.26]^{a}	50	0.34 [0.24–0.40]^{b}	42	0.53 [0.43–0.59]^{c}	21	<0.001
TTFE (m/s)	0.50 [0.45–0.59]^{a}	50	0.51 [0.42–0.57]^{a}	42	0.78 [0.68–0.85]^{b}	20	<0.001
TTFA (m/s)	0.54 ± 0.16^{a}	50	0.66 ± 0.20^{b}	42	0.63 ± 0.24 ^{ab}	20	0.005
RV E:E′	4.72 [4.00–5.78]^{a}	50	5.54 [4.21–6.42]^{a}	41	7.70 [5.73–9.62]^{b}	20	<0.001
Peak PA velocity (m/s)	0.89 [0.78–0.98]^{a}	50	0.82 [0.69–0.94]^{a}	40	0.73 [0.62–0.98]^{a}	24	0.192
AT (ms)	76.0 [69.0–82.0]^{a}	50	53.5 [45.0–64.5]^{b}	40	48.0 [40.3–52.3]^{b}	24	<0.001
AT:RVET	0.43 [0.40–0.46]^{a}	50	0.33 [0.30–0.39]^{b}	40	0.31 [0.27–0.34]^{b}	24	<0.001
LVIDDN	1.46 ± 0.15^{a}	50	1.55 ± 0.37^{a}	43	1.17 ± 0.55^{b}	24	0.002
TMFE (m/s)	0.68 [0.58–0.77]^{a}	50	0.68 [0.56–0.93]^{a}	43	0.58 [0.48–0.97]^{a}	21	0.614
TMFA (m/s)	0.60 [0.53–0.70]^{a}	50	0.76 [0.62–0.90]^{b}	43	0.72 [0.61–0.89] ^{ab}	21	0.002
MV sep S′ (cm/s)	9.0 [8.1–12.4]^{a}	50	9.1 [7.3–10.2] ^{ab}	43	7.7 [7.1–9.4]^{b}	19	0.038
MV sep E′ (cm/s)	8.7 [7.3–10.4]^{a}	50	8.2 [6.0–9.4] ^{ab}	43	7.2 [6.2–8.2]^{b}	19	0.031
MV sep A′ (cm/s)	7.9 [6.8–9.5]^{a}	50	8.2 [6.6–11.1]^{a}	43	6.4 [5.3–7.8]^{b}	19	0.009
MV lat S′ (cm/s)	11.9 [9.7–13.4]^{a}	50	11.3 [9.6–13.5]^{a}	36	12.5 [10.8–13.7]^{a}	16	0.656
MV lat E′ (cm/s)	10.0 [8.9–12.7]^{a}	50	8.9 [7.6–10.7]^{b}	36	11.0 [7.6–13.2] ^{ab}	16	0.034
MV lat A′ (cm/s)	9.5 [7.5–11.8]^{a}	50	10.0 [8.6–12.7]^{a}	36	9.0 [7.7–10.5]^{a}	16	0.252

Values with different superscripted letters (a, b and c) indicate significant differences between groups ($p<0.0167$).

Ao, aorta; AT, acceleration time; AT:RVET, ratio of AT to the right ventricular ejection time; CVC, caudal vena cava; FAC, fractional area change; lat, lateral; LD, longest diameter of the caudal vena cava area; LD max, longest diameter of the maximal caudal vena cava area during expiration; LD min, longest diameter of the minimal caudal vena cava area during inspiration; LVIDDN, normalized left ventricular internal dimension at end-diastole; MV, mitral valve; MV A′, peak velocity of diastolic mitral annular motion as determined by pulsed-wave Doppler; MV E′, peak velocity of early diastolic mitral annular motion as determined by pulsed-wave Doppler; MV S′, peak velocity of systolic mitral annular motion as determined

by pulsed-wave Doppler; NA, not applicable; nTAPSE, normalized tricuspid annular plane systolic excursion; PA, pulmonary artery; PR, pulmonary regurgitation; RA, right atrium; RHD, right-sided heart disease; RV, right ventricular; RV A′, peak velocity of diastolic tricuspid annular motion as determined by pulsed-wave Doppler; RV E:E′, ratio of the peak velocity of early diastolic transtricuspid to peak velocity of early diastolic tricuspid annular motion as determined by pulsed-wave Doppler; RV E′, peak velocity of early diastolic tricuspid annular motion as determined by pulsed-wave Doppler; RV S′, peak velocity of systolic tricuspid annular motion as determined by pulsed-wave Doppler; RVTX, right ventricular Tei index; SD, shortest diameter perpendicular to the LD of the caudal vena cava area; SD/LD (max), ratio of SD max to LD max; SD max, shortest diameter perpendicular to the longest diameter of the maximal caudal vena cava area during expiration; SD max/Ao, ratio of SD max to Ao diameter; SD min, shortest diameter perpendicular to the longest diameter of the minimal caudal vena cava area during inspiration; SD/LD (min), ratio of SD min to LD min; SD min/Ao, ratio of SD min to Ao diameter; sep, septal; TAPSE, tricuspid annular plane systolic excursion; TMFA, peak velocity of late transmitral flow; TMFE, peak velocity of early diastolic transmitral flow; TR, tricuspid regurgitation; TTFA, peak velocity of late transtricuspid flow; TTFE, peak velocity of early diastolic transtricuspid flow.

and the ratio of SD to LD (SD/LD), have been used to estimate CVP in paediatric patients and have been reported to be less influenced by body weight than by the absolute diameter of the CVC, which increases as a child grows [41—43]. Our study revealed that the SD(min)/Ao and SD/LD(min) showed the highest accuracy among all ratios for identifying R-CHF in various-sized dogs with RHD. To our knowledge, ultrasonographic assessment of the CVC in dogs with RHD has been performed only through a subjective evaluation of CVC enlargement, and an objective evaluation using diagnostic standard values has not been reported [44]. Therefore, this is the first study to report that SD/LD and ratio of SD to Ao diameter would be useful variables for evaluating venous congestion in dogs.

The RA area index, TTFE, and RVTX were higher in dogs with RHD with R-CHF than without R-CHF. The RA area index in dogs has been reported to be associated with the presence of R-CHF [20]. The RA area has been shown to be strongly correlated with the BSA in healthy dogs and humans [20,45]. Thus, normalisation of the RA area to the BSA (i.e., RA area index) has been recommended [20,45]. The median and range of the RA area index in healthy dogs derived from our study (median, 7.55 cm^2/m^2; range, 5.39—9.23 cm^2/m^2) were similar to those in the previous study (median, 7.3 cm^2/m^2; range, 4.2—10.2 cm^2/m^2) [20]. In our study, the RA area index identified the presence of R-CHF with high accuracy. This finding was consistent with the previous report [20].

With respect to the index of myocardial performance for assessing systolic and diastolic function, RVTX was positively correlated with pulmonary vascular resistance in dogs and humans with PH [18,46]. Increases in TTFE have reportedly been associated with severity of TR in humans [47]. In our study, 75% of dogs with RHD with R-CHF had severe TR compared to only 20% of dogs with RHD without R-CHF. Therefore, higher TTFE in dogs with RHD with R-CHF than in dogs with RHD without R-CHF might have been due to more severe TR cases in dogs with RHD with R-CHF. No previous study has investigated whether RVTX or TTFE is a useful echocardiologic index for identifying the presence of R-CHF in dogs. Our results suggest that RVTX and TTFE would be useful echocardiographic variables to identify the presence of R-CHF in dogs with RHD.

Several limitations of our study should be noted. First, we did not evaluate RV function with right-sided heart catheterisation, which is necessary for making a definitive diagnosis of R-CHF. Second, the dual pulsed-wave Doppler used for the measurement of RVTX currently has limited application and is not widely available, although previous studies

have demonstrated good agreement in RVTX measurements between dual pulsed-wave Doppler and conventional Doppler [38,48]. Third, our study included dogs that had received cardiac medications before study enrolment. The cardiac meditations could have influenced the volume status and echocardiographic variables. The medication history did not significantly differ between dogs with RHD with R-CHF and dogs with RHD without R-CHF. Thus, the results of statistical analyses may not have been influenced by medication history. Fourth, all measurements were made with the dogs positioned in left lateral recumbency. It has been reported that the IVC diameter is influenced by patient positioning in humans (i.e., left lateral recumbency creates the smallest diameter, right lateral recumbency creates the largest diameter, and dorsal recumbency provides intermediate values for IVC measurement) [44,45]. The effect of patient positioning on the CVC diameter in dogs has not been investigated. Thus, patient positioning during CVC diameter measurements should be taken into consideration when interpreting the results. Fifth, we noted a significant difference in body weight among the groups in our study. Previous studies in dogs and humans reported that Ao and CVC diameters were influenced by body weight [30,49]. Our study showed that both Ao and CVC diameters positively correlated with body weight. Therefore, the differences in these variables among the groups may be due to the difference of body weight. On the other hand, ratio of IVC diameter to Ao diameter and SD/LD are reported to be less influenced by body weight [42,50]. Similarly, ratio of CVC diameter and Ao diameter and SD/LD were not corelated with body weight in our study and were highest in dogs with RHD with R-CHF. Sixth, Darnis et al. (2018) reported that the inter-operator repeatability of the ratio of SD to Ao diameter in healthy dogs was poor [30]. Our results were not affected by inter-operator variability because only one sonographer performed all ultrasonographic and echocardiographic examinations. However, the inter-operator repeatability of the CVC variables in dogs needs to be assessed to accurately conduct the measurements.

Conclusions

In addition to the echocardiographic assessment of right-sided heart function, this study revealed that ultrasonographic CVC variables, such as SD(min)/Ao and SD/LD(min), could be useful for identifying the presence of R-CHF in dogs with RHD.

Conflicts of Interest Statement

The authors declare no conflicts of interest.

Supplementary data

Supplementary data to this article can be found online at https://doi.org/10.1016/j.jvc.2021.01.005.

References

[1] Carluccio E, Biagioli P, Alunni G, Murrone A, Zuchi C, Coiro S, Riccini C, Mengoni A, D'Antonio A, Ambrosio G. Prognostic value of right ventricular dysfunction in heart failure with reduced ejection fraction: superiority of longitudinal strain over tricuspid annular plane systolic excursion. Circ Cardiovasc Imag 2018;11:e006894.

[2] Cho JH, Kutti Sridharan G, Kim SH, Kaw R, Abburi T, Irfan A, Kocheril AG. Right ventricular dysfunction as an echocardiographic prognostic factor in hemodynamically stable patients with acute pulmonary embolism: a meta-analysis. BMC Cardiovasc Disord 2014;14:64.

[3] Damy T, Kallvikbacka-Bennett A, Goode K, Khaleva O, Lewinter C, Hobkirk J, Nikitin NP, Dubois-Randé JL, Hittinger L, Clark AL, Cleland JG. Prevalence of, associations with, and prognostic value of tricuspid annular plane systolic excursion (TAPSE) among out-patients referred for the evaluation of heart failure. J Card Fail 2012;18:216—25.

[4] Dini FL, Conti U, Fontanive P, Andreini D, Banti S, Braccini L, De Tommasi SM. Right ventricular dysfunction is a major predictor of outcome in patients with moderate to severe mitral regurgitation and left ventricular dysfunction. Am Heart J 2007;154:172—9.

[5] Guazzi M, Bandera F, Pelissero G, Castelvecchio S, Menicanti L, Ghio S, Temporelli PL, Arena R. Tricuspid annular plane systolic excursion and pulmonary arterial systolic pressure relationship in heart failure: an index of right ventricular contractile function and prognosis. Am J Physiol Heart Circ Physiol 2013;305:1373—81.

[6] Sabe MA, Sabe SA, Kusunose K, Flamm SD, Griffin BP, Kwon DH. Predictors and prognostic significance of right ventricular ejection fraction in patients with ischemic cardiomyopathy. Circulation 2016;134:656—65.

[7] Venner C, Selton-Suty C, Huttin O, Erpelding ML, Aliot E, Juillière Y. Right ventricular dysfunction in patients with idiopathic dilated cardiomyopathy: prognostic value and predictive factors. Arch Cardiovasc Dis 2016;109:231—41.

[8] Nakamura K, Morita T, Osuga T, Morishita K, Sasaki N, Ohta H, Takiguchi M. Prognostic value of right ventricular tei index in dogs with myxomatous mitral valvular heart disease. J Vet Intern Med 2016;30:69—75.

[9] Kaye BM, Borgeat K, Mõtsküla PF, Luis Fuentes V, Connolly DJ. Association of tricuspid annular plane systolic excursion with survival time in boxer dogs with ventricular arrhythmias. J Vet Intern Med 2015;29:582—8.

[10] Schober KE, Hart TM, Stern JA, Li X, Samii VF, Zekas LJ, Scansen BA, Bonagura JD. Detection of congestive heart failure in dogs by Doppler echocardiography. J Vet Intern Med 2010;24:1358—68.

[11] Serres F, Chetboul V, Tissier R, Sampedrano CC, Gouni V, Nicolle AP, Pouchelon JL. Chordae tendineae rupture in dogs with degenerative mitral valve disease: prevalence, survival, and prognostic factors (114 cases, 2001—2006). J Vet Intern Med 2007;21:258—64.
[12] Borgarelli M, Savarino P, Crosara S, Santilli RA, Chiavegato D, Poggi M, Bellino C, La Rosa G, Zanatta R, Haggstrom J, Tarducci A. Survival characteristics and prognostic variables of dogs with mitral regurgitation attributable to myxomatous valve disease. J Vet Intern Med 2008;22:120—8.
[13] Nakamura K, Kawamoto S, Osuga T, Morita T, Sasaki N, Morishita K, Ohta H, Takiguchi M. Left atrial strain at different stages of myxomatous mitral valve disease in dogs. J Vet Intern Med 2017;31:316—25.
[14] Kim JH, Park HM. Usefulness of conventional and tissue Doppler echocardiography to predict congestive heart failure in dogs with myxomatous mitral valve disease. J Vet Intern Med 2015;29:132—40.
[15] Caivano D, Rishniw M, Birettoni F, Patata V, Giorgi ME, Dei K, Porciello F. Right ventricular outflow tract fractional shortening: an echocardiographic index of right ventricular systolic function in dogs with pulmonary hypertension. J Vet Cardiol 2018;20:354—63.
[16] Chapel EH, Scansen BA, Schober KE, Bonagura JD. Echocardiographic estimates of right ventricular systolic function in dogs with myxomatous mitral valve disease. J Vet Intern Med 2018;32:64—71.
[17] Cunningham SM, Aona BD, Antoon K, Rush JE, Barton BA. Echocardiographic assessment of right ventricular systolic function in Boxers with arrhythmogenic right ventricular cardiomyopathy. J Vet Cardiol 2018;20:343—53.
[18] Morita T, Nakamura K, Osuga T, Yokoyama N, Morishita K, Sasaki N, Ohta H, Takiguchi M. Changes in right ventricular function assessed by echocardiography in dog models of mild RV pressure. Echocardiography 2017;34:1040—9.
[19] Morita T, Nakamura K, Osuga T, Morishita K, Sasaki N, Ohta H, Takiguchi M. Right ventricular function and dyssynchrony measured by echocardiography in dogs with precapillary pulmonary hypertension. J Vet Cardiol 2019;23:1—14.
[20] Vezzosi T, Domenech O, Iacona M, Marchesotti F, Zini E, Venco L, Tognetti R. Echocardiographic evaluation of the right atrial area index in dogs with pulmonary hypertension. J Vet Intern Med 2018;32:42—7.
[21] Vezzosi T, Domenech O, Costa G, Marchesotti F, Venco L, Zini E, Del Palacio MJF, Tognetti R. Echocardiographic evaluation of the right ventricular dimension and systolic function in dogs with pulmonary hypertension. J Vet Intern Med 2018;32:1541—8.
[22] Miryam M, Reems MA. Central venous pressure: principles, measurement, and interpretation. Compend Contin Educ Vet 2012;34:E1.
[23] Haddad F, Doyle R, Murphy DJ, Hunt SA. Right ventricular function in cardiovascular disease, part II: pathophysiology, clinical importance, and management of right ventricular failure. Circulation 2008;117:1717—31.
[24] Nelson NC, Drost WT, Lerche P, Bonagura JD. Noninvasive estimation of central venous pressure in anesthetized dogs by measurement of hepatic venous blood flow velocity and abdominal venous diameter. Vet Radiol Ultrasound 2010;51:313—23.
[25] Ciozda W, Kedan I, Kehl DW, Zimmer R, Khandwalla R, Kimchi A. The efficacy of sonographic measurement of inferior vena cava diameter as an estimate of central venous pressure. Cardiovasc Ultrasound 2016;14:33.
[26] Beigel R, Cercek B, Luo H, Siegel RJ. Noninvasive evaluation of right atrial pressure. J Am Soc Echocardiogr 2013;26:1033—42.
[27] De Vecchis R, Baldi C, Giandomenico G, Di Maio M, Giasi A, Cioppa C. Estimating right atrial pressure using ultrasounds: an old issue revisited with new methods. J Clin Med Res 2016;8:569—74.
[28] Pellicori P, Carubelli V, Zhang J, Castiello T, Sherwi N, Clark AL, Cleland JG. IVC diameter in patients with chronic heart failure: relationships and prognostic significance. JACC Cardiovasc Imag 2013;6:16—28.
[29] Seo Y, Iida N, Yamamoto M, Machino-Ohtsuka T, Ishizu T, Aonuma K. Estimation of central venous pressure using the ratio of short to long diameter from cross-sectional images of the inferior vena cava. J Am Soc Echocardiogr 2017;30:461—7.
[30] Darnis E, Boysen S, Merveille AC, Desquilbet L, Chalhoub S, Gommeren K. Establishment of reference values of the caudal vena cava by fast-ultrasonography through different views in healthy dogs. J Vet Intern Med 2018;32:1308—18.
[31] Kwak J, Yoon H, Kim J, Kim M, Eom K. Ultrasonographic measurement of caudal vena cava to aorta ratios for determination of volume depletion in normal beagle dogs. Vet Radiol Ultrasound 2018;59:203—11.
[32] Meneghini C, Rabozzi R, Franci P. Correlation of the ratio of caudal vena cava diameter and aorta diameter with systolic pressure variation in anesthetized dogs. Am J Vet Res 2016;77:137—43.
[33] Kellihan HBSR. Pulmonary hypertension in dogs: diagnosis and therapy. Vet Clin North Am Small Anim Pract 2010;40:623—41.
[34] Francis AJ, Johnson MJS, Culshaw GC, Corcoran BM, Martin MWS, French AT. Outcome in 55 dogs with pulmonic stenosis that did not undergo balloon valvuloplasty or surgery. J Small Anim Pract 2011;52:282—8.
[35] Hedman K, Nylander E, Henriksson J, Bjarnegård N, Brudin L, Tamás É. Echocardiographic characterization of the inferior vena cava in trained and untrained females. Ultrasound Med Biol 2016;42:2794—802.
[36] Visser LC, Scansen BA, Schober KE, Bonagura JD. Echocardiographic assessment of right ventricular systolic function in conscious healthy dogs: repeatability and reference intervals. J Vet Cardiol 2015;17:83—96.
[37] Poser H, Berlanda M, Monacolli M, Contiero B, Coltro A, Guglielmini C. Tricuspid annular plane systolic excursion in dogs with myxomatous mitral valve disease with and without pulmonary hypertension. J Vet Cardiol 2017;19:228—39.
[38] Morita T, Nakamura K, Osuga T, Lim SY, Yokoyama N, Morishita K, Sasaki N, Ohta H, Takiguchi M. Repeatability and reproducibility of right ventricular Tei index valves derived from three echocardiographic methods for evaluation of cardiac function in dogs. Am J Vet Res 2016;77:715—20.
[39] Cornell CC, Kittleson MD, Della Torre P, Häggström J, Lombard CW, Pedersen HD, Vollmar A, Wey A. Allometric scaling of M-mode cardiac measurements in normal adult dogs. J Vet Intern Med 2004;18:311—21.
[40] Rudski LG, Lai WW, Afilalo J, Hua L, Handschumacher MD, Chandrasekaran K, Solomon SD, Louie EK, Schiller NB. Guidelines for the echocardiographic assessment of the right heart in adults: a report from the American Society of echocardiography. Endorsed by the European association of echocardiography, a registered branch of the European Society of Cardiology, and the Canadian Society of Echocardiograpy. J Am Soc Echocardiogr 2010;23:685—713.

[41] Chen L, Hsiao A, Langhan M, Riera A, Santucci KA. Use of bedside ultrasound to assess degree of dehydration in children with gastroenteritis. Acad Emerg Med 2010;17:1042—7.
[42] Sato Y, Kawataki M, Hirakawa A, Toyoshima K, Kato T, Itani Y, Hayakawa M. The diameter of the inferior vena cava provides a noninvasive way of calculating central venous pressure in neonates. Acta Paediatr Int J Paediatr 2013;102:e241—6.
[43] Sharareh B, Azita B, Masoud MR. A comparison between the bedside sonographic measurements of the inferior vena cava indices and the central venous pressure while assessing the decreased intravascular volume in children. Adv Biomed Res 2018;25:97.
[44] Reinero C, Visser LC, Kellihan HB, Masseau I, Rozanski E, Clercx C, Williams K, Abbott J, Borgarelli M, Scansen BA. ACVIM consensus statement guidelines for the diagnosis, classification, treatment, and monitoring of pulmonary hypertension in dogs. J Vet Intern Med 2020;34:549—73.
[45] Grünig E, Henn P, D'Andrea A, Claussen M, Ehlken N, Maier F, Naeije R, Nagel C, Prange F, Weidenhammer J, Fischer C, Bossone E. Reference values for and determinants of right atrial area in healthy adults by 2-dimensional echocardiography. Circ Cardiovasc Imag 2013;6:117—24.
[46] Ogihara Y, Yamada N, Dohi K, Matsuda A, Tsuji A, Ota S, Ishikura K, Nakamura M, Ito M. Utility of right ventricular Tei-index for assessing disease severity and determining response to treatment in patients with pulmonary arterial hypertension. J Cardiol 2014;63:149—53.
[47] Lancellotti P, Moura L, Pierard LA, Agricola E, Popescu BA, Tribouilloy C, Hagendorff A, Monin JL, Badano L, Zamorano JL. European Association of Echocardiography recommendations for the assessment of valvular regurgitation. Part 2 : mitral and tricuspid regurgitation (native valve disease). Eur J Echocardiogr 2010;11:307—32.
[48] Choi JO, Choi JH, Lee HJ, Noh HJ, Huh J, Kang IS, Lee HJ, Lee SC, Kim DK, Park SW. Dual pulsed-wave Doppler tracing of right ventricular inflow and outflow: single cardiac cycle right ventricular Tei index and evaluation of right ventricular function. Kor Circ J 2010;40:391—8.
[49] Nakao S, Come PC, Mckay RG, Ransil BJ. Effect of positional changes on inferior vena caval size and dynamics and correlations with right-sided cardiac pressure. Am J Cardiol 1987;59:125—32.
[50] Gui J, Zhou B, Liu J, Ou B, Wang Y, Jiang L, Tang W, Luo B, Yang Z. Impact of body characteristics on ultrasound-measured inferior vena cava parameters in Chinese children. Braz J Med Biol Res 2019;52:e8122.